Time-Resolved Spectroscopy and Scaling Behavior in $LiCl/H_2O$ near the Liquid-Glass Transition

I. C. Halalay[1],[a] and Keith A. Nelson[2]

[1]*Department of Physics, Massachusetts Institute of Technology, Cambridge, Massachusetts 02139*
[2]*Department of Chemistry, Massachusetts Institute of Technology, Cambridge, Massachusetts 02139*
(Received 31 July 1991)

Time-domain light scattering experiments on ps–μs time scales have been conducted on a concentrated aqueous LiCl solution. Analysis of mechanical and electrical modulus spectra confirms some results of mode-coupling theory: simple scaling for α peaks and property-independent power laws. This is made without any assumptions about the data which are not derived from theory. A new characteristic time scale, reflecting the short- and intermediate-range ordering dynamics, is also observed.

PACS numbers: 64.70.Pf, 65.70.+y, 78.47.+p

During the past decade the study of the liquid-glass transition has taken a new impetus, sparked by the emergence of new theoretical and experimental approaches [1]. Of great interest is the mode-coupling theory (MCT) [2–5] which has generated a new way of thinking about this difficult problem. Traditionally, the emphasis in the analysis of susceptibility data has been on the different relaxation peaks. MCT shifts the focus to the wings and to the minimum between the α and β relaxations, for which it makes quantitative predictions. Their experimental verification requires measurements over many decades in time scale. Large bandwidth electrical susceptibility measurements have been possible for decades, but mechanical measurements in the MHz–GHz range (relevant to MCT) have been difficult. We present here impulsive stimulated light scattering (ISS) data from an aqueous LiCl solution, as well as a novel analysis of mechanical and electrical susceptibility data for supercooled liquids.

Descriptions of the theoretical underpinnings of the ISS technique and its experimental implementations are given elsewhere [6,7]. Briefly, two $\lambda_L = 1064$ nm, 100 ps, parallel polarized laser pulses crossed at an angle θ_E were used for transient grating excitation of both longitudinal acoustic waves and the thermal diffusion mode at the grating wave vector $q = (4\pi/\lambda_L)\sin(\theta_E/2)$. The time-dependent diffraction of a variably delayed 532-nm probe pulse was then measured. We used seven scattering angles between 1° and 60°, yielding acoustic wavelengths of 62.8, 30.8, 14.1, 7.53, 3.96, 1.94, and 1.07 μm and frequencies from 25 MHz to 4 GHz. The electrolyte $LiCl/H_2O$ 13 mol% was studied for $70 < T < 300$ K. This concentration is situated between the equilibrium (12.5 mol%) and the lower nonequilibrium (14.5 mol%) eutectic concentrations [8]. The calorimetric glass transition temperature is $T_g = 135$ K.

Typical ISS data are displayed in Fig. 1. All exhibit damped acoustic oscillations (the transient response to sudden heating) and a steady-state density modulation (caused by thermal expansion at grating maxima and compression at nulls) which decays due to thermal diffusion. The trends in acoustic frequency and attenuation rate are as expected and observed in other glass-forming materials [9]. Between 165 and 200 K the steady-state response shows additional temporal features. There is a gradual rise in signal, which can be thought of as time-dependent thermal expansion and which reflects slow components of structural relaxation in the viscoelastic fluid (observed much more dramatically in several other materials [9]). After this rise is a decay on a time scale much faster than thermal diffusion, which has not been observed in other materials or other concentrations of $LiCl/H_2O$. Data at all temperatures in this interval fit the functional form

$$I(t) \sim \{A[e^{-\Gamma_H t} - e^{-\Gamma_A t}\cos(\omega_A t)] + B[e^{-\Gamma_1 t} - e^{-\Gamma_2 t}]\}^2, \quad (1)$$

with Γ_H the grating decay rate due to thermal diffusion, and Γ_A and ω_A the acoustic attenuation rate and frequency, respectively. Γ_1 and Γ_2 are parameters for an overdamped oscillator model which gives a good description of the gradual rise and decay in signal. The unusual behavior occurs at all scattering angles and its characteristic time scale is wave-vector independent. We believe that it reflects the dynamics of short-range ordering in the liquid. Its absence in other concentrations of $LiCl/H_2O$ suggests that it may be related to specific coordination geometries of H_2O around Li. A recent solution of the dispersion equation for a mode-coupling model describing supercooled liquids [10] may provide additional insights: Besides modes predicted by linearized hydrodynamics [11], there appears a wave-vector-independent relaxational mode. Values of Γ_1^{-1} and Γ_2^{-1} will be reported subsequently; both increase from ~ 1 ns to ~ 1 μs and the temperature is reduced from 200 to 165 K. Typical thermal diffusivity values ($\kappa_T = \Gamma_H/q^2$) are 1.7×10^{-7} m/s^2 for $150 < T < 300$ K, increasing to 4.0×10^{-7} m/s^2 at 100 K. For $T < 165$ K and $T > 200$ K the diffracted signal is well described by a functional form without the overdamped oscillator in Eq. (1). Our analysis makes use of the acoustic parameters, which determine the complex compressibility modulus $M(\omega)$.

Figure 2 shows the imaginary part of the mechanical modulus, given by

$$M''(\omega) = (\rho/q^2)(2\omega_A\Gamma_A), \quad (2)$$

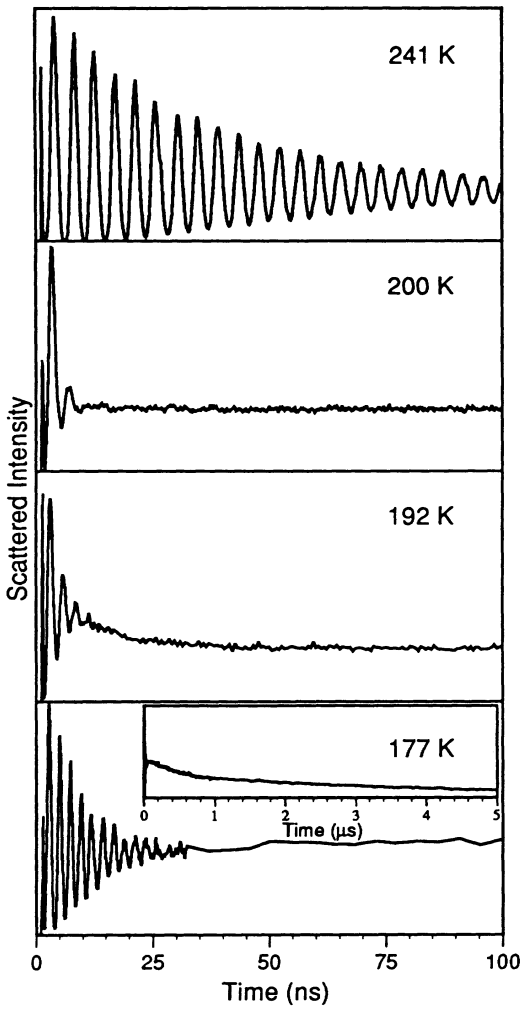

FIG. 1. ISS data scans for $LiCl/H_2O$ 13 mol% for an excitation angle $\theta_E = 8.10°$. The sweeps illustrate all temporal features: damped acoustic oscillations at short times, time-dependent thermal expansion at intermediate times, time-dependent contraction at somewhat longer times, and thermal diffusion at the longest times.

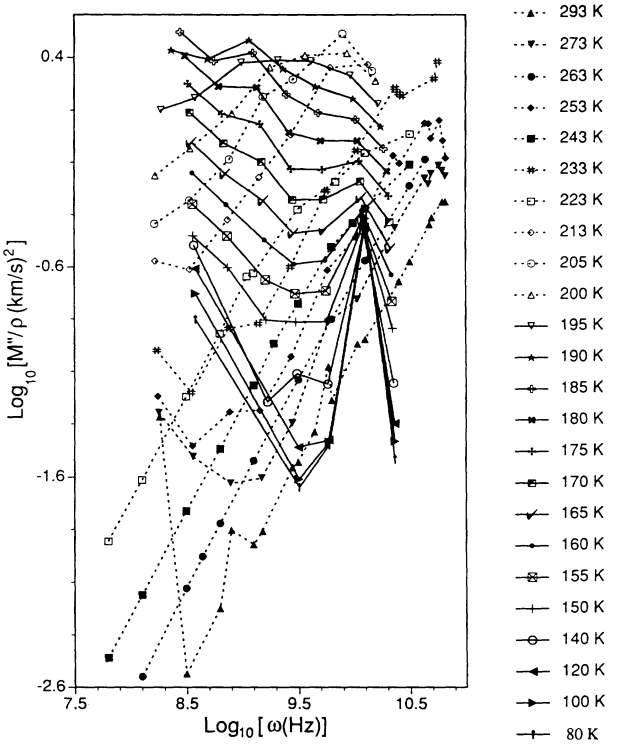

FIG. 2. Imaginary part of the complex compressibility modulus divided by the density $M''(\omega)/\rho$, for $LiCl/H_2O$ 13 mol%. The modulus values above $\omega = 20$ GHz, at 233, 253, 273, and 293 K, were obtained through Brillouin scattering [12] in a 12.5 mol% $LiCl/H_2O$ solution. All the values for 223, 243, and 253 K as well as part of the values at 293 K were determined from ultrasonic and Brillouin scattering experiments in a 12.2 mol% $LiCl/H_2O$ solution [13].

as a function of frequency at various temperatures (ρ is the mass density). The maximum of $M''(\omega)$ is within our experimental frequency window at 190–200 K. At higher (lower) temperatures, the maximum is beyond the high- (low-) frequency end of our dynamic range and we observe the low- (high-) frequency side of the α peak. At temperatures below 175 K a minimum and a second peak (at about 10 GHz) become apparent. At the lowest frequencies ($\omega < 0.3$ GHz) and highest temperatures ($T > 250$ K) the acoustic attenuation rates are very low and systematic errors are difficult to avoid [6]. The apparent rise in M'' at the lowest frequencies and highest temperatures hence cannot be considered reliable.

MCT describes both the slow α relaxation and the faster β relaxation. The main theoretical effort so far consists in the solution of a nonlinear integro-differential equation for the density-density correlation function. The solution is extremely difficult and has been found both analytically and numerically in various approximations [2–5]. Factorization of wave-vector and time dependences in a correlation function F_{AB} is a key ansatz of MCT:

$$F_{AB}(q,t) = f^c_{AB} + h_{AB}(q)\mathcal{G}(t)\,, \tag{3}$$

with f^c_{AB} a nonergodicity parameter, $h_{AB}(q)$ a critical amplitude, and $\mathcal{G}(t)$ a scaling function. Since $\mathcal{G}(t)$ does not depend on observables A or B, different measurements should yield the same functional form. This means that various susceptibilities $\chi(\omega) \sim \omega\mathcal{G}(\omega)$ must have identical frequency dependences.

Fourier transformation of the solution shows that $\chi''(\omega)$ has two peaks (centered on ω_α and ω_β, $\omega_\alpha \ll \omega_\beta$). The high- ($\omega_\alpha < \omega$) and low- ($\omega < \omega_\beta$) frequency asymptotic solutions in the supercooled liquid (for the α and β peaks, respectively) obey the following power laws:

$$\chi''(\omega) \sim \omega^{-b}, \omega^a\,. \tag{4}$$

The exponents a and b are determined from the so-called exponent parameter λ:

$$\lambda = \frac{\Gamma^2(1-a)}{\Gamma(1-2a)} = \frac{\Gamma^2(1+b)}{\Gamma(1+2b)}, \quad (5)$$

where Γ in Eq. (5) is the gamma function. MCT also predicts $\chi''(\omega < \omega_a) \sim \omega^{1.0}$ on the low-frequency side of the α peak [5] and a scaling law for the value of the susceptibility minimum which occurs at some frequency ω^* between the α and β peaks:

$$\chi''(\omega^*) \sim |T - T_c|^{1/2}. \quad (6)$$

T_c is a crossover temperature at which the amplitude ratio of the β peak to the α peak has a maximum. Relations (4)–(6) are testable through measurements of susceptibilities as a function of frequency and temperature.

We use complex compressibility modulus data, determined from ISS, Brillouin scattering [12,13], and ultrasonics [13], as well as electrical modulus data [14] to test these results. Our analysis involves no empirical relaxation functional forms, extrapolations to determine the low-frequency $M_0(T)$ and high-frequency $M_\infty(T)$ limiting values of the moduli, or interpolations between values of $M(\omega)$ determined at widely different frequencies (to connect gaps of one or more decades in ω). We use a log-log representation for $M''(\omega)$ so that power-law behavior yields straight lines and the multiplicative factor needed to superimpose dielectric and mechanical modulus values (which have different units) becomes an additive constant accounted for by a mere vertical shift. To compare electrical and mechanical moduli, we normalize the master plots such that $\omega_{\text{peak}} = 1$ and $M''(\omega_{\text{peak}}) = 1$. All the points from Fig. 2 (except those from the lowest five temperatures, at which the frequency-dependent data contain only one point in the α relaxation region) are included in the α relaxation scaling plot of Fig. 3.

Figure 3 shows the rescaled longitudinal elastic modulus spectrum in the low-frequency relaxation region (α peak), obtained by shifting the separate plots for $150 < T < 293$ K (displayed in Fig. 2) parallel to the abscissa and normalized as described above. The differences in heights between the ultrasonic (at 223 and 243 K) and the ISS scaled α relaxation peaks is due to the strong variations with concentration in the acoustic attenuation and speed of sound at these temperatures [15,16]. Plotted on the same graph are data for the imaginary part of the electrical modulus in the temperature interval 143–167 K [14], similarly rescaled and adjusted vertically to overlap with the mechanical modulus data. The high-frequency wing follows a power law ($M'' \sim \omega^{-b}$) with values of the exponent $b_{\text{mech}} = 0.28$ and $b_{\text{el}} = 0.26$ in excellent agreement. For $b = 0.28$, Eq. (5) yields $\lambda = 0.91$ which indicates a strong coupling between charge and mass fluctuations [3]. At the highest frequencies and lowest temperatures deviations from the simple scaling are apparent. Figure 2 indicates for each temperature below approximately 170 K a clear change in the frequency dependence of M''. At these low temperatures the β relaxation may be approaching our experimentally

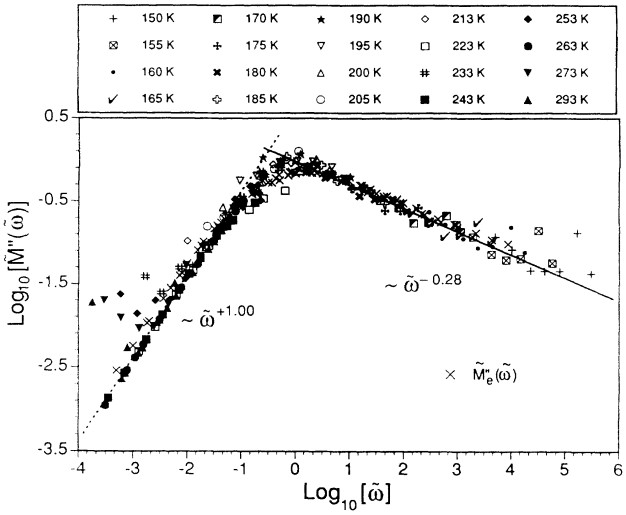

FIG. 3. Master plot for the imaginary part of the compressibility modulus in LiCl/H_2O 13 mol%. The symbols are identical with those in Fig. 2. Also shown (× symbols) are electrical modulus values for LiCl/H_2O 12.95 mol% [14]. Power-law behavior obtains on both sides of the α peak. The moduli show identical scaling behavior, as predicted.

accessible frequency range. Figure 2 also shows a "spike" at about 10 GHz for low temperatures ($T < 175$ K), whose origin is uncertain and which we are investigating further in our laboratory. Independent of this narrow feature, however, the end of the high-frequency wing of the α relaxation peak appears to have been reached in the low-temperature data. Finally, the low-frequency side of the α peak also appears to follow a power law ($M'' \sim \omega^x$) with exponents $x_{\text{mech}} = 0.89$ and $x_{\text{el}} = 0.97$, in agreement with uncertainties and close to the MCT prediction of 1.00.

From the scaling procedure we obtain characteristic relaxation times $\tau(T)$, displayed in Fig. 4. Their relative values are determined by the extent of the translation along the abscissa. The absolute time scale is set by the peak frequency $\omega_p = 2\pi/\tau$ at a temperature for which the maximum in $M''(\omega)$ is the center of the experimentally available frequency window ($\omega_p = 2.10$ GHz at 195 K for M''_m, $\omega_p = 785$ kHz at 155 K for M''_e). A common fit by the Vogel-Tammann-Fulcher form $\tau = \tau_0 \exp[B/(T - T_0)]$ yields parameters $B = 1482$ K, $T_0 = 99$ K, and $\tau_0 = 4.6$ fs.

In summary, ISS experiments combined with Brillouin scattering and ultrasonics data have permitted the determination of the complex compressibility modulus in a concentrated LiCl/H_2O solution over a frequency range of 2–3 decades in the MHz–GHz region. A new characteristic time scale was observed in the ISS data, which may reflect relaxation dynamics of the local structure in the supercooled liquid. The predictions of simple scaling and identical power laws for different susceptibilities in the α peak region were confirmed by mechanical and

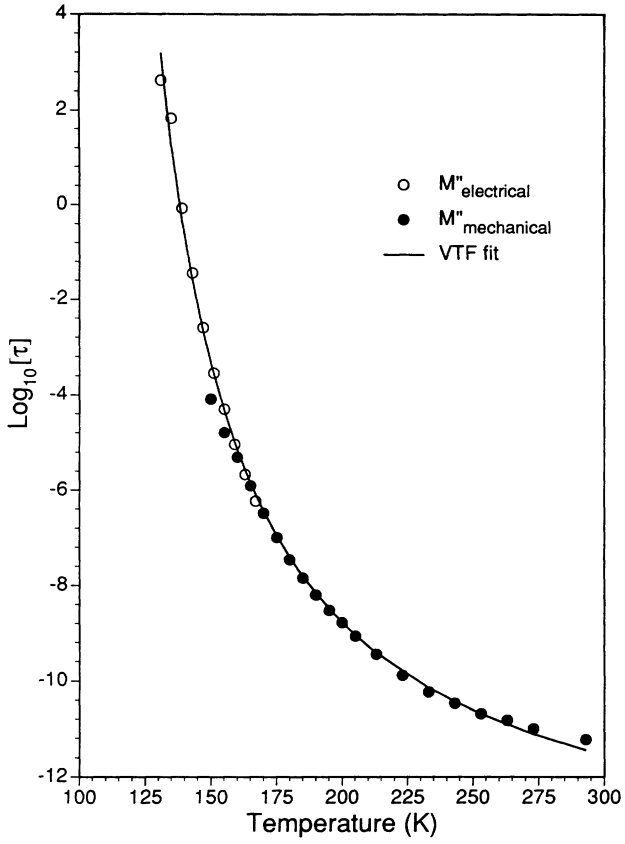

FIG. 4. Characteristic relaxation times $\tau(T)$ determined through the scaling procedure for the mechanical and electrical moduli, together with a common Vogel-Tammann-Fulcher fit, yielding parameters $B=1482$ K, $T_0=99$ K, and $\tau_0=4.6$ fs.

electrical modulus data. MCT may not yet provide quantitatively correct predictions for all the features observed in various materials, but it has nonetheless provided incisive guidance by pointing to the types of scaling relations which should be sought. Our results can in turn provide assistance for further refinements of the theory describing the liquid-glass transition in more complicated systems.

This work was supported in part by NSF Grant No. DMR-9002279 and by contributions from du Pont and Perkin-Elmer. One of the authors (I.C.H.) was supported by a General Motors Fellowship.

[a]Current address: Physical Chemistry Department, General Motors Research and Environmental Staff, Warren, MI 48090.

[1] For recent progress see J. Non-Cryst. Solids **131-133** (1991); *Basic Features of the Glassy State,* edited by J. Colmenero and A. Alegria (World Scientific, Singapore, 1989).

[2] U. Bengtzelius, W. Götze, and A. Sjölander, J. Phys. C **17**, 5915 (1984).

[3] W. Götze and L. Sjögren, J. Phys. Condens. Matter **1**, 4183 (1989); **1**, 4203 (1989); W. Götze, *ibid.* **2**, 8485 (1990).

[4] L. Sjögren, Z. Phys. B **79**, 5 (1990).

[5] W. Götze and L. Sjögren, J. Phys. C **21**, 3407 (1988); W. Götze (private communication).

[6] X.-Y. Yan and K. A. Nelson, J. Chem. Phys. **87**, 6240 (1987); **87**, 6257 (1987).

[7] L. T. Cheng, Ph.D. thesis, Massachussetts Institute of Technology, 1987 (unpublished); S. M. Silence, Ph.D. thesis, Massachusetts Institute of Technology, 1991 (unpublished).

[8] P. Chieux, in *The Physics and Chemistry of Aqueous Ionic Solutions,* edited by M.-C. Bellissent-Funel and G. W. Neilson (Reidel, Dordrecht, Netherlands, 1987), p. 359.

[9] X.-Y. Yan, L.-T. Cheng, and K. A. Nelson, J. Chem. Phys. **88**, 6477 (1988); S. M. Silence, S. R. Goates, and K. A. Nelson, Chem. Phys. **149**, 233 (1990); A. R. Duggal and K. A. Nelson, J. Chem. Phys. **94**, 7677 (1991).

[10] J. Schofield and I. O. Oppenheim, Physica (Amsterdam) A (to be published).

[11] R. Balescu, *Equilibrium and Nonequilibrium Statistical Mechanics* (Wiley, New York, 1974), p. 427.

[12] K. G. Breitschwerdt and E. Polke, Chem. Phys. Lett. **73**, 196 (1980); Ber. Bunsenges. Phys. Chem. **85**, 1059 (1981).

[13] G. Kasper and K. Tamm, J. Chem. Phys. **72**, 5279 (1980).

[14] C. T. Moynihan, R. D. Bressel, and C. A. Angell, J. Chem. Phys. **55**, 4414 (1971).

[15] J. Pelous, A. Essabouri, and R. Vacher, J. Phys. (Paris), Colloq. **46**, C8-665 (1985).

[16] N. J. Tao, G. Li, and H. Z. Cummins, Phys. Rev. B **43**, 5815 (1991).